

Preparation and up-conversion luminescence of 8 nm rare-earth doped fluoride nanoparticles

V.K. Tikhomirov^{1*}, M. Mortier², P. Gredin², G. Patriarche³, C. Görller-Walrand^{4*}, and V.V. Moshchalkov¹

¹ INPAC-Institute for Nanoscale Physics and Chemistry, Katholieke Universiteit Leuven, Belgium

² Laboratoire de Chimie de la Matière Condensée, UMR CNRS 7574, Ecole Nationale Supérieure de Chimie de Paris, France

³ Laboratoire de Photonique et Nanostructure, Marcoussis, France

⁴ Chemistry Department, Katholieke Universiteit Leuven, Belgium

*Corresponding authors: Victor.Tikhomirov@fys.kuleuven.be, Christiane.Walrand@chem.kuleuven.be

Abstract: Free-standing, 8 nm diameter, rare-earth doped nanoparticles $\text{Re}_{10}\text{Pb}_{25}\text{F}_{65}$ have been prepared, where Re stands for either single rare-earth ion, such as Er^{3+} , Yb^{3+} , Eu^{3+} , Dy^{3+} , Ho^{3+} , Tm^{3+} or combinations of those ions. The nanoparticles have been extracted by chemical etching from the oxyfluoride nano-glass-ceramics template and analyzed by transmission electron microscope with energy dispersion spectroscopy. The nanoparticles show durable up-conversion photoluminescence, which is neither concentration nor impurity quenched after 6 months ageing in ambient atmosphere. High doping levels in these nanoparticles ensure high, up to 15%, quantum yield of up-conversion luminescence.

©2008 Optical Society of America

OCIS codes: (160.5690) Rare earth doped materials; (160.4236) Nanomaterials; (250.5230) Photoluminescence.

References and links

1. L. Aigouy, P. Lalanne, J. P. Hugonin, G. Juliè, V. Mathet, and M. Mortier, "Near-field analysis of surface waves launched at nano-slit apertures," *Phys. Rev. Lett.* **98**, 153902 (2007).
2. B. Steitz, Y. Axmann, H. Hofmann, and A. Petri-Fink, "Optical properties of annealed Mn^{2+} doped ZnS nanoparticles," *J. Lumin.* **128**, 92-99 (2008).
3. H. Zhou, M. Wissinger, J. Fallert, R. Hauschild, F. Stelzl, C. Klingshirn, and H. Kalt, "Ordered, uniform-sized ZnO nanolaser arrays," *Appl. Phys. Lett.* **91**, 181112 (2007).
4. J. Zhang, Y. Fu, and J. R. Lakowicz, "Luminescent images of single gold nanoparticles and their labeling on silica beads," *Opt. Express* **15**, 13415-13420 (2007).
5. D. Matsuura, "Red, green and blue up-conversion luminescence of trivalent rare earth ion-doped Y_2O_3 nanocrystals," *Appl. Phys. Lett.* **81**, 4528-4528 (2002).
6. F. Auzel, "Up-conversion and anti-Stokes processes with d and f ions in solids," *Chem. Rev.* **105**, 139-173 (2004).
7. J. F. Suyver, J. Grimm, M. K. van Veen, D. Biner, K. W. Krämer, and H. U. Güdel, "Upconversion spectroscopy and properties of NaYF_4 doped with Er^{3+} , Tm^{3+} and/or Yb^{3+} ," *J. Lumin.* **117**, 1-12 (2006).
8. V. K. Tikhomirov, D. Furniss, I. M. Reaney, M. Beggiora, M. Ferrari, M. Montagna, and R. Rolli, "Fabrication and characterization of nanoscale, Er^{3+} -doped, ultratransparent oxyfluoride glass-ceramics," *Appl. Phys. Lett.* **81**, 1937-1939 (2002).
9. V. K. Tikhomirov, K. Driesen, C. Görller-Walrand, and M. Mortier, "Broadband telecommunication wavelength emission in Yb^{3+} - Er^{3+} - Tm^{3+} co-doped nano-glass-ceramics," *Opt. Express* **15**, 9535-9540 (2007).
10. M. Mortier and G. Patriarche, "Oxide glass used as inorganic template for fluorescent fluoride nano-particle synthesis," *Opt. Mater.* **28**, 1401-1409 (2006).
11. V. D. Rodríguez, V. K. Tikhomirov, J. Méndez-Ramos, J. del-Castillo, and C. Görller-Walrand, "Measurement of quantum yield of up-conversion luminescence in Er^{3+} -doped nano-glass-ceramics," *J. Nanosci. Nanotechnol.* **8**, 1-4 (2008).
12. D. J. M. Bevan, J. Strähle, and O. Greis, "The crystal structure of tveitite, an ordered yttrifluorite mineral," *J. Solid State Chem.* **44**, 75-81 (1982).
13. A. Ikesue, Y. L. Aung, T. Taira, T. Kamimura, K. Yoshida, and G. L. Messing, "Progress in ceramics lasers," *Annu. Rev. Mater. Sci.* **36**, 397-429 (2006).

14. J. Méndez-Ramos, V. K. Tikhomirov, V. D. Rodríguez, and D. Furniss, "Infrared tuneable up-conversion phosphor based on Er^{3+} -doped nano-glass-ceramics," *J. Alloys Compd.* **440**, 328-334 (2007).
 15. H. Desirena, E. De la Rosa, A. Shulzgen, S. Shabet, and N. Peyghambarian, " Er^{3+} and Yb^{3+} concentration effect in the spectroscopic properties and energy transfer in $\text{Yb}^{3+}/\text{Er}^{3+}$ codoped tellurite glasses," *J. Phys. D: Appl. Phys.* **41**, 095102 (2008).
-

1. Introduction

The luminescent nanoparticles have recently attracted a lot of interest for a broad range of photonic applications, i.e. near-field microscopy, including thermal sensing, detection of surface plasmon polariton (SPP) waves; nano-lasers, nano-phosphors, biological nano-labels and other, e.g. [1-5] and refs therein. Rare-earth doping of the nanoparticles results in luminescence bands from UV to IR part of the spectrum, including multi-colour up-conversion luminescence bands [5-7]. For many applications the frequency up-conversion photoluminescence of nanoparticles is required, i.e. for detection of SPP, infrared nano-phosphors, nano-lasers, nano-labels and other nano-sensors [1,5-7].

The preparation technique of the rare-earth doped nanoparticles has to ensure that the nanoparticles are regular and homogeneous in shape, size, and chemical composition (optimally, spherically shaped with a diameter, often, of about 10 nm or less), and possess high quantum yield luminescence. In this work, we have prepared $\text{Re}_{10}\text{Pb}_{25}\text{F}_{65}$ nanoparticles (Re stands for the rare-earth ion), which satisfy these requirements, and in particular show high yield of up-conversion luminescence due to a high doping level and low phonon energy in these nanoparticles.

2. Experimental and results

First, the bulk oxyfluoride rare-earth doped nano-glass-ceramics template $32(\text{SiO}_2)9(\text{AlO}_{1.5})31.5(\text{CdF}_2)18.5(\text{PbF}_2)5.5(\text{ZnF}_2):3.5(\text{ReF}_3)$, mol%, has been prepared as described elsewhere [8], where Re stands for Er^{3+} , Yb^{3+} , Eu^{3+} , Dy^{3+} , Ho^{3+} , Tm^{3+} or some combinations of these ions, e.g. in [9]. The Re ions nucleate the growth of PbF_2 -based crystalline nanoparticles in this nano-glass-ceramics template and therefore up to 90 to 100% of Re ions are incorporated into these nanoparticles [8-10] and refs therein. Further the nanoparticles have been extracted from the nano-glass-ceramics template by means of chemical etching of the template with 40% hydrofluoric acid and subsequent precipitation from the solution in a rotating centrifuge [10]. The nanoparticles have been aggregated in nanopowders of about 0.4 g weight and have been further kept either in air atmosphere or in vacuum in sealed ampoules.

The shape, size and chemical composition of the nanoparticles have been studied by transmission electron microscope with energy dispersion spectroscopy (TEM EDS). The time resolved luminescence spectra were measured by using the excitation with 5 ns pulses of optical parametric oscillator (OPO) operating at about 975 nm. An integration sphere has been used for the estimation of quantum yield of steady state up-conversion photoluminescence when pumped with CW laser diode at 975 nm. Another method used for the estimation of the quantum yield in this paper is based on measurements of pump power dependence of the resonant luminescence; it is described in [11].

Figure 1 shows one of the TEM images of the nanoparticles, doped in this case with Dy^{3+} , (a) and respective selected area electron diffraction pattern (b). All nanoparticles in this particular case and also all nanoparticles doped with other rare-earth ions are round shaped and have a diameter of about 8 ± 1 nm. An approximate chemical composition for all dopant cases approaches $\text{Re}_{10}\text{Pb}_{25}\text{F}_{65}$ within accuracy of 10%, as found from the energy dispersive spectra of scattered electrons. Traces of Cd up to 3 at% and of O up to 6 at% have been detected in some selected areas. These impurities were not regular and their concentration varied substantially from area to area so that they were not intrinsic to the nanoparticles and, therefore, located most probably at their surface. They may be present due to not complete etching and reaction with water and oxygen from the atmosphere, respectively. No amorphous phases have been observed in all cases, as seen in Fig. 1(b), where the diffraction pattern

corresponds to the face-centered cubic fluorite lattice, e.g. [8,12]. Apparently, the chemical formula $\text{Re}_{10}\text{Pb}_{25}\text{F}_{65}$ is similar to the formula of the naturally occurred stoichiometric crystal of tveitite type $\text{Re}_x\text{Pb}_{1-x}\text{F}_{2+x}$ (at $x \approx 0.3$), which has a slightly distorted face-centered fluorite type structure typical of $\beta\text{-CaF}_2$ and/or $\beta\text{-PbF}_2$ [12]. In this stoichiometric crystal, the dopants are dissolved homogeneously and therefore do not form clusters. This results in a high absorption coefficient and prevents concentration quenching of luminescence in nanoparticles, as discussed below.

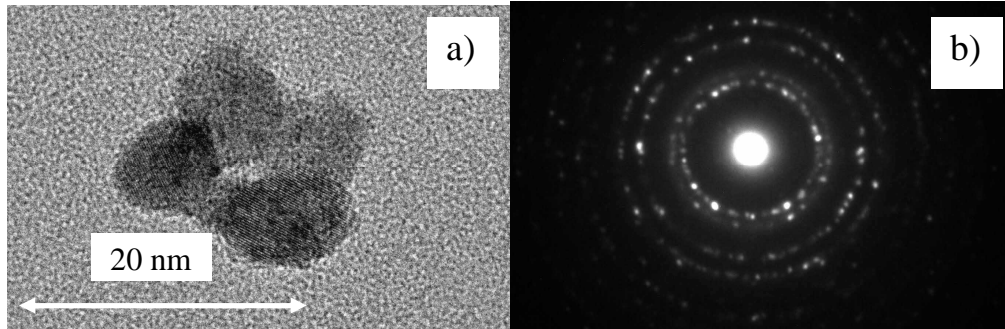


Fig. 1. High resolution transmission electron microscope image (a) and selected area electron diffraction pattern (b) obtained from the Dy^{3+} -doped nanoparticles of approximate composition $\text{Dy}_{10}\text{Pb}_{25}\text{F}_{65}$.

Figure 2 shows visible absorption spectra of about 0.3 mm thick and 5 mm diameter pellets made from Ho^{3+} -doped nanoparticles in ambient atmosphere by pressing at 1 ton for 30 min (thin blue line) and 5 ton for 30 min (thick red line).

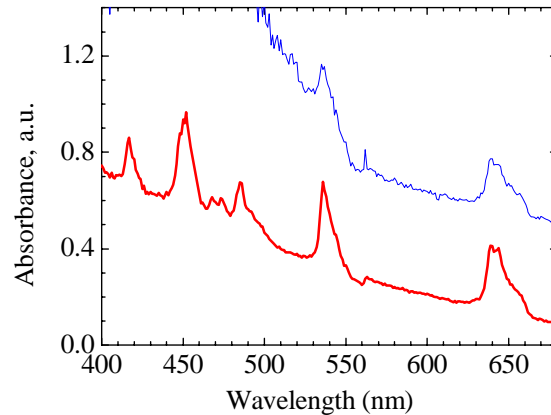


Fig. 2. Absorbance spectra of 0.3 mm thick pellet made of Ho^{3+} -doped nanoparticles at 1 ton pressing for 30 minutes (thin blue line) and 5 ton pressing for 30 minutes (thick red line). The peaks in spectra correspond to absorption bands of Ho^{3+} .

As seen from Fig. 2, the pellets are translucent and their translucency and absorption coefficient in Ho^{3+} absorption bands increase with pressing magnitude. This indicates the formation of a dense structure of the pellets and that the dopants are well dissolved and optically active in the nanoparticles. The translucency itself suggests a potential for producing transparent lasing ceramics by pressing these crystalline nanoparticles, which is also facilitated by their cubic structure [13].

Figure 3 shows time resolved up-conversion luminescence spectra taken on Er^{3+} -doped (a) and Yb^{3+} - Er^{3+} co-doped (b) crystalline nanopowders. Other up-conversion luminescence

bands were substantially weaker; therefore we do not show them in these graphs. The $\text{Yb}^{3+}/\text{Er}^{3+}$ ratio equals to 6 in case (b). The quantum yield for the up-conversion luminescence, [11], was found to be about 1% and 15% in Er^{3+} -doped and Yb^{3+} - Er^{3+} co-doped nanopowders, respectively, when pumped by CW laser diode operating at 975 nm wavelength and pump power density of 20 W/cm^2 , as in case of Fig. 3.

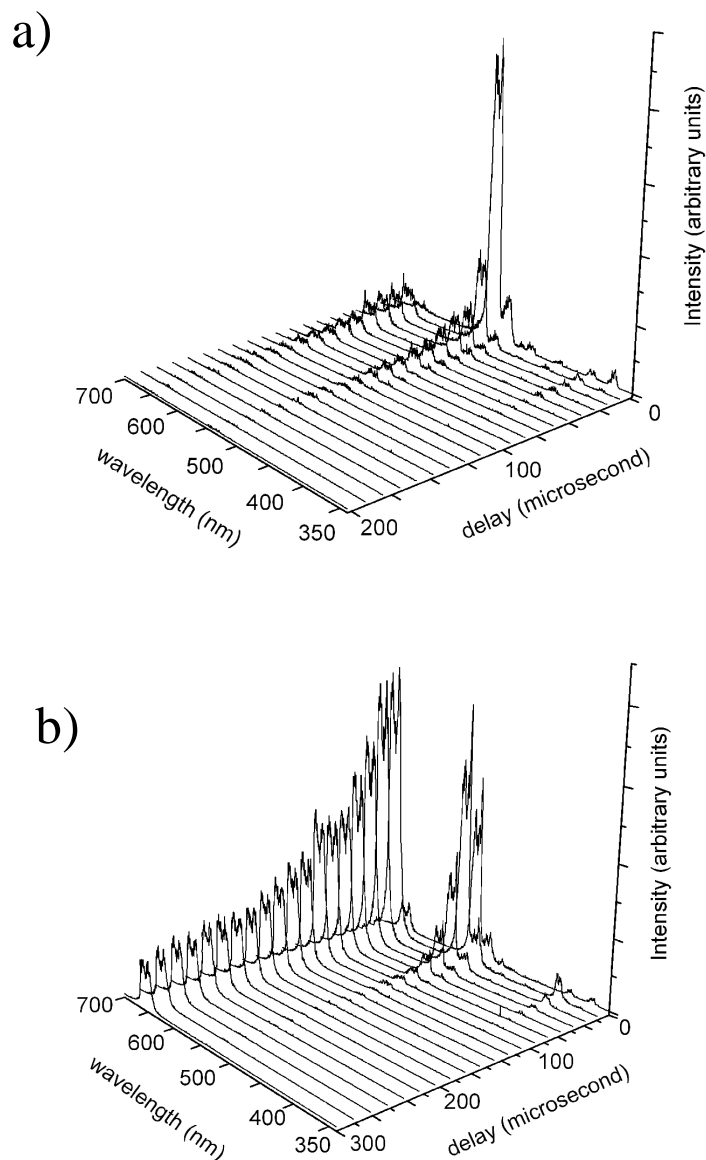


Fig. 3. Time resolved up-conversion luminescence spectra taken on crystalline nanopowders $\text{Re}_{10}\text{Pb}_{25}\text{F}_{65}$, where Re stands for dopant Er^{3+} (a) and co-dopants Yb^{3+} - Er^{3+} (b). The emission was excited by OPO laser at 975 nm, 5 ns pulse duration and 10 Hz pulse repetition rate. Delay (microsecond) represents time after single excitation pulse. The laser was focused on the powder placed in a Pyrex ampoule sealed under vacuum resulting in pump power of 20 W/cm^2 .

3. Discussion

Energy level diagram of Er^{3+} and Yb^{3+} ions in Fig. 4 shows possible routes for the excitation of up-conversion luminescence in single Er^{3+} -doped sample, Fig. 3(a), and in Er^{3+} - Yb^{3+} co-doped sample, Fig. 3(b), when pumped at 975 nm in absorption bands of Er^{3+} and Yb^{3+} , respectively [6,7,14,15]. While only the Er^{3+} absorbs in the former case, the Yb^{3+} mostly absorbs in the latter case since the absorption cross-section for Yb^{3+} is order of magnitude higher than for Er^{3+} [6,7,15] and also because concentration of Yb^{3+} ions is 6 times higher in Er^{3+} - Yb^{3+} co-doped sample. Note that at such high doping level as 10 at.%, Fig. 3, the *energy transfer (ET)* two- and three- photon processes (shown in Fig. 4 by dashed lines) dominate in the excitation of up-conversion luminescence, while excited state absorption (ESA) two-photon processes are of minor importance [14,15]. In this respect, *high doping level* defines mechanism of up-conversion luminescence presented in Fig. 3.

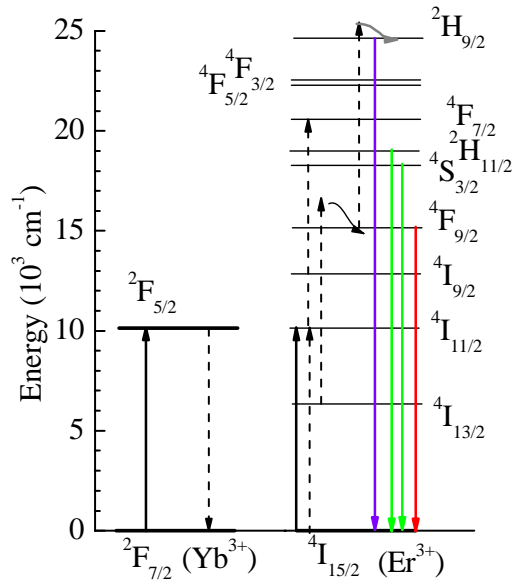


Fig. 4. Energy level diagram of Er^{3+} and Yb^{3+} . Excitation and emission transitions are showed by solid up- and down-headed arrows, respectively. Dash lines show energy transfer processes between Yb^{3+} and Er^{3+} ions, which result in up-conversion luminescence of Er^{3+} [7,14,15]. Wavy solid lines show phonon emission processes required for matching excitation quanta with the respective energy levels of Er^{3+} .

It is seen in Fig. 3(a) that the red (650 nm) up-conversion luminescence band of Er^{3+} has been substantially quenched in single Er^{3+} -doped sample, while it has a long lifetime of about 260 μs in the Er^{3+} - Yb^{3+} co-doped sample, Fig. 3(b). The 260 μs lifetime is similar to the lifetime of Er^{3+} -dopants in the nano-glass-ceramics template [10,14], which was used for extraction of nanoparticles., indicative that this red band has not been affected by extraction of Er^{3+} - Yb^{3+} co-doped nanoparticles from the template.

On the other hand, it is clearly seen in Figs. 3(a,b) that the green (550 nm) up-conversion luminescence band of Er^{3+} has been substantially quenched in both the single Er^{3+} -doped sample and in the Er^{3+} - Yb^{3+} co-doped sample. In both cases of Fig. 3(a) and Fig. 3(b), the lifetime of this green emission band is about 40 μs ., which is order of magnitude shorter than in the respective nano-glass-ceramics templates [10,14]. This indicates that this green band of Er^{3+} has been significantly affected by the extraction of Er^{3+} -doped nanoparticles from the template.

To understand how the subtraction of nanoparticles from the template may affect luminescence of nanoparticles, we note here that TEM EDS studies (Fig. 1) indicated presence of oxygen on the surface of nanoparticles, which might easily combine with hydrogen resulting in OH radical, which has vibration energy as high as 3400 cm^{-1} . This OH impurity is known to quench luminescence from the levels of rare-earth ions by emission of phonons with energy of 3400 cm^{-1} [6,7,14,15].

The green and red luminescence bands in Fig. 3 occurs from the levels $^4\text{S}_{3/2}$, $^2\text{H}_{11/2}$ and $^4\text{F}_{9/2}$ of Er^{3+} , respectively (see diagram in Fig. 4), and therefore these bands can be efficiently quenched by OH impurities in single Er^{3+} -doped sample, Fig. 3(a), since only emission of 1 or 2 phonons with energy 3400 cm^{-1} is required to bridge the gap between the $^4\text{S}_{3/2}$, $^2\text{H}_{11/2}$ and $^4\text{F}_{9/2}$ and the next lower lying levels of Er^{3+} .

Certainly, one option to avoid quenching of up-conversion luminescence of Er^{3+} by OH impurities would be to stay away from any contaminations related to the OH radicals in extraction process of nanoparticles; this study is underway. However, very fortunately, in the Yb^{3+} - Er^{3+} co-doped nanoparticles, the red up-conversion luminescence is still not quenched by OH, Fig. 3(b). The reason for that proposed here is that the lifetime of the red emission band (or $^4\text{F}_{9/2}$ level) of Er^{3+} in Yb^{3+} - Er^{3+} co-doped nanoparticles is defined by dynamics of the energy transfer from Yb^{3+} co-dopants to Er^{3+} co-dopants rather than by lifetime of the $^4\text{F}_{9/2}$ level itself. This can be understood from diagram in Fig. 4 assuming that the energy transfer process, which populates the $^4\text{F}_{9/2}$ level of Er^{3+} , corresponds to $(^2\text{F}_{5/2}, ^4\text{I}_{13/2}) \rightarrow (^2\text{F}_{7/2}, ^4\text{F}_{9/2}) - \hbar\omega$. $\hbar\omega$ is the total energy of phonons released/absorbed in this energy transfer process and it is indicated by wavy arrow from the $^4\text{F}_{9/2}$ level in Fig. 4. A dominance of this energy transfer process in up-conversion luminescence of heavy doped samples has been reported, e.g. in [14,15] and refs therein.

The gap between $^2\text{F}_{5/2}$ and $^2\text{F}_{7/2}$ levels of Yb^{3+} is rather large at about 10000 cm^{-1} , therefore the $^2\text{F}_{5/2}$ level of Yb^{3+} cannot be quenched efficiently by emission of the 3400 cm^{-1} phonons via OH radicals, and therefore dynamics of the energy transfer process $(^2\text{F}_{5/2}, ^4\text{I}_{13/2}) \rightarrow (^2\text{F}_{7/2}, ^4\text{F}_{9/2}) - \hbar\omega$ is not substantially affected by OH resulting in a strong up-conversion luminescence with a long lifetime from the $^4\text{F}_{9/2}$ level of Er^{3+} in Yb^{3+} - Er^{3+} co-doped nanoparticles, in agreement with data of Fig. 3(b). Ageing of Er^{3+} and Yb^{3+} - Er^{3+} co-doped nanoparticles in atmosphere for 6 months did not affect parameters of their up-conversion luminescence.

4. Conclusion

High quantum yield up-conversion luminescence has been observed in Yb^{3+} - Er^{3+} co-doped 8 nm nanoparticles $(\text{Yb,Er})_{10}\text{Pb}_{25}\text{F}_{65}$ (Yb/Er ratio equals 6) prepared by chemical extraction from nano-glass-ceramics template. The 8 nm nanoparticles heavily doped with other rare-earth ions, such as Yb^{3+} , Eu^{3+} , Dy^{3+} , Ho^{3+} , Tm^{3+} or combinations of those ions, have also been obtained by the same method. The up-conversion luminescence of these nanoparticles, especially of Yb^{3+} - Er^{3+} co-doped nanoparticles, has a potential for applications, e.g. in near-field microscopy, including thermal nano-sensing, detection of surface plasmon polariton (SPP) waves; nano-lasers, nano-phosphors, biological nano-labels.

Acknowledgments

The work in Leuven has been supported by the Research Fund K.U.Leuven GOA, Flemish FWO, and Belgian IAP projects.